IL NUOVO CIMENTO **47 C** (2024) 259
DOI 10.1393/ncc/i2024-24259-8

COMMUNICATIONS: SIF Congress 2023

Excitons at room temperature in a two-dimensional quantum spin Hall insulator(*)

A. CONSIGLIO

Institut für Theoretische Physik und Astrophysik and Würzburg-Dresden Cluster of Excellence ct.qmat, Universität Würzburg - 97074 Würzburg, Germany

received 31 January 2024

Summary. — Both experimental techniques and theoretical methods based on density functional theory, ab-initio *GW*, and Bethe-Salpeter equation calculations have been employed to investigate optical resonances in the quantum spin Hall (QSH) insulator Bismuthene (a honeycomb layer of bismuth atoms) grown on a Silicon Carbide substrate. This material exhibits a direct gap of 1.3 eV at the K and K' points, making it an excellent candidate for studying excitons in the visible and near-infrared range, even under room temperature conditions. The results, here focused on the theoretical aspects, confirm that the strong electron-hole interaction indeed has a significant impact on the optical excitations, and provide the first evidence of excitons in a 2D QSH insulator. Two main excitonic transitions are observed, with the lowest peak embedded in the single-particle direct gap, featuring a binding energy of ~ 0.15 eV. Furthermore it is noteworthy that, in this material, both excitonic and topological features stem from the same electronic structure.

1. – Introduction

Excitons are bound electron-hole pairs formed through Coulomb interaction. These quasi-particles garner significant scientific interest, serving as focal points for extensive research not only addressing fundamental scientific questions but also exploring practical applications such as energy transfer in devices like solar cells and LEDs [2]. Remarkably, excitons possess indeed the capability to transport energy without conveying a net electric charge. Their importance is particularly evident in two-dimensional materials, where enhanced Coulomb interactions and correlations have unveiled a diverse array of many-body states like non-hydrogenic Rydberg series of excitons [3]. The observation of excitons in a room-temperature large-gap QSH insulator [1], specifically Bismuthene on Silicon Carbide (Bi:SiC) [4], marks a compelling progress into the intersection of excitonic physics and topological electronic properties.

(*) This article is a theoretical overview of ref. [1].

Commonly studied pristine monolayer Transition Metal Dichalcogenides (TMDCs) such as WS_2, WSe_2, MoS_2, $MoSe_2$, and $MoTe_2$ in their 2H-phase, fall indeed into the category of topologically trivial insulators.

The interplay between optical selection rules and topology is thus expected to stimulate numerous future experimental and theoretical investigations from a fundamental standpoint. Until now, experimental investigations of the impact of non-trivial global band topology on light-matter interaction and exciton physics has been hindered by the absence of suitable topological insulators with a wide enough band gap for coupling to high-energy photons. Only recently 2D topological insulators like 1T′-WTe_2 monolayers [5] and Bi:SiC, an atomically thin bismuth layer arranged in a graphene-like unbuckled honeycomb lattice [4, 6] (fig. 1(a)), have been discovered and synthesized.

In Bi:SiC, the Spin-Orbit Coupling (SOC) induced by heavy Bi atoms and the orbital filtering resulting from covalent bonding to the substrate, which also breaks the inversion symmetry of the system, lead to the emergence of a substantial topological band gap (figs. 1(b), (c), (d) and 2), accessible to optical spectroscopy in the near-infrared. This sets bismuthene apart from previously known topological insulators and presents novel experimental opportunities for studying photo-induced exciton physics in 2D topological materials.

2. – Methods

The first-principle study started with the determination of the system's equilibrium geometry, via ionic relaxation, in the framework of Density Functional Theory (DFT). Specifically, the calculations have been performed with the Quantum Espresso package [7]. Norm-conserving pseudo-potentials have been used, and the wave functions are expanded in plane-waves with an energy cut-off of 40 Ry, large enough to guarantee converged results. Exchange-correlation effects are included using the Perdew-Burke-Ernzerhof (PBE) functional [8]. The Brillouin zone has been sampled with a $12 \times 12 \times 1$

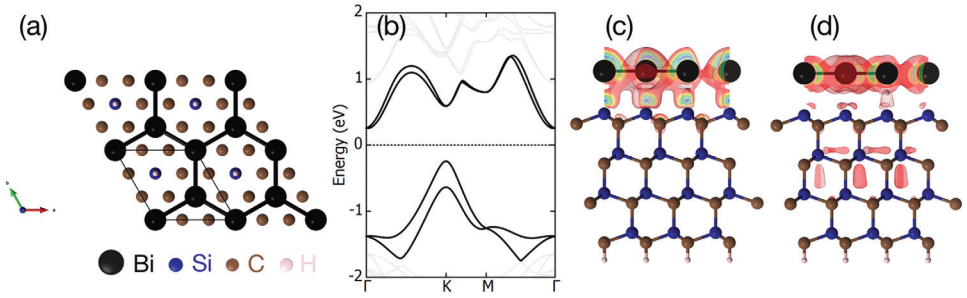

Fig. 1. – (a) Top-view of the 2×2 Bi:SiC cell. The bismuthene hexagonal net, as well as the unit cell, have been highlighted. (b) DFT-GGA band structure of Bi:SiC, including SOC. The two top-most valence eigenvalues and the two lowest conduction eigenvalues along the high-symmetry path Γ-K-M-Γ have been highlighted. These states are the most important for the optical transitions. (c) Charge density isosurface computed for the topmost valence band. Note that the charge is mainly localized on the bismuthene layer, mostly with $p_x + p_y$ character. (d) Charge density isosurface computed for the lowest conduction band. Also in this case the charge is mainly localized on the bismuthene layer, except for a certain contribution coming from the SiC substrate around the M point (see also fig. 2(c)).

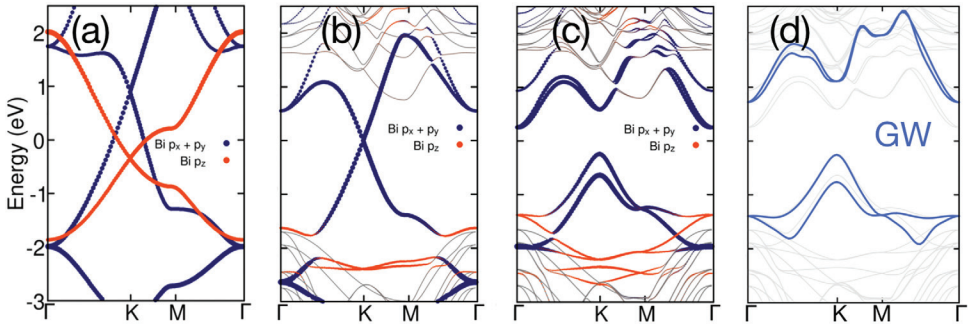

Fig. 2. – (a) DFT-GGA band structure without SOC and without SiC substrate. The character coming from bismuth's p orbitals has been highlighted. p_z orbitals form a graphene-like net and electronic structure. (b) DFT-GGA band structure without SOC, with the SiC substrate being included. The substrate strongly binds to the p_z orbital imposing an orbital filtering mechanism and removing them from low energies close to the Fermi level. (c) DFT-GGA band structure with SOC and with SiC substrate. SOC contributes with two distinct terms: an intrinsic, atomic one, responsible for the opening of the gap at the Fermi level, and as a Rashba contribution associated with the breaking of inversion symmetry, due to the substrate. The latter contribution leads to a pronounced splitting of the two top-most valence bands at K/K'. (d) Comparison between the DFT-GGA band structure (faded light-grey lines) and the band structure including G_0W_0 corrections.

grid, both for self-consistent and non self-consistent calculations. Finally, spin-orbit coupling has been included self-consistently.

The unit cell is composed by one Bismuthene layer and four layers of Silicon Carbide substrate (figs. 2(a), (c), (d)).

Considering a big enough number of SiC layers in this case is of pivotal importance, as it provides an accurate determination of the low-energy electronic structure, as well as of the screening properties. The importance of the latter point is particularly evident when considering GW calculations, where DFT results are enhanced by replacing the exchange-correlation potential with the many-body self-energy Σ (see figs. 2(c) and (d)). The self-energy is here obtained as a product of the one-body Green's function G, describing the propagation of a particle in the system, and the dynamically screened Coulomb interaction W [9-12]. The W has been here computed within the random phase approximation, including local field effects. While increasing the number of substrate layers, preserving the same amount of vacuum along the z-direction, the energy gap has to decrease, as a consequence of the increased dielectric screening. It is hence required to carefully assure the convergence of the results respect to the substrate thickness, in our case corresponding to 4 layers.

Finally, in addition to the GW outcomes, the impact of electron-hole interactions is accounted for through the solution of the Bethe-Salpeter Equation (BSE) for the electron-hole amplitude [13-15], and the excitonic two-body wave function is expressed as a product of occupied and unoccupied orbitals. The GW+BSE calculations have been performed using the YAMBO package [16, 17].

Due to the strong localization of the exciton at the K/K$'$ point (see figs. 3(b) and (c)), it has been necessary to increase the k-grid up to $24 \times 24 \times 1$ for the many-body calculations, before reaching converged results.

Geometries and charge density iso-surfaces have been visualized with VESTA [18].

3. – Results

In order to obtain meaningful many-body results for the absorption spectrum, it is important to start from a suitable single-particle description. For this reason, aware of the DFT likelihood to underestimate the band gap, we relied on *GW* electronic calculations for Bi:SiC.

The *GW* band structure for Bi:SiC is shown in fig. 2(d), as solid light-blue lines superimposed to the light-gray DFT bands. These bands are characterized by a strong Rashba-splitting at the valleys and by an indirect electronic band gap, between the valence band at K and the conduction band at Γ of $E_{\text{ind}} = 0.97\,\text{eV}$.

The direct single-particle gap at the K (K′) point, relevant for the optical transitions, is equal to $E_{\text{direct}} = 1.36$ eV in the *GW* approximation.

On top of this, the optical spectrum is affected by the relevant Coulomb coupling between electrons and holes, generated by photo-excitation. The theoretical analysis of the two-particle properties and consequent excitation spectrum are hence obtained solving the Bethe-Salpeter equation for the electron-hole amplitude,

$$(E_{c\mathbf{k}} - E_{v\mathbf{k}})A_{vc\mathbf{k}} + \sum_{v'c'\mathbf{k}'} \langle vc\mathbf{k}|K_{eh}|v'c'\mathbf{k}'\rangle A_{v'c'\mathbf{k}'} = \Omega A_{vc\mathbf{k}}. \tag{1}$$

The electronic excitations are described within the framework of electron-hole pairs, characterized by quasi-particle energies $E_{v\mathbf{k}}$ and $E_{c\mathbf{k}}$ in the valence and conduction bands, respectively. The coefficients $A_{vc\mathbf{k}}$ represent the exciton contributions in the electron-hole basis, and Ω denotes the eigen-energies. The kernel K_{eh} incorporates the screened Coulomb interaction between electrons and holes, along with the exchange interaction. Additionally, local field effects arising from the optical excitations of periodically arranged atomic orbitals in Bi:SiC are taken into account [19].

The absorption spectra, presented in fig. 3(a), illustrate the comparison between the calculations with and without electron-hole interactions. This enables to extract the excitonic binding energy, approximately of 0.15 eV for the lowest peak. The value is determined measuring the difference between the independent particle *GW* absorption gap E_{direct}, and the energy position of the first peak. In the same fig. 3(a), around 1.7 eV, it is possible to note a prominent second peak. Its energy shift aligns with the Rashba splitting observed in the valence states at the K and K′ valleys.

This leads to a notable separation between the first and second excitonic peaks, ultimately resulting in the merging of the latter into the continuum of electron-hole excitations. Depending on the coupling strength between the second exciton peak and the continuum, this merging may give rise to a Fano resonance.

Finally, the convergence issue anticipated in the Methods section arises due to the extended nature of Wannier-Mott type excitons in Bi:SiC. Figure 3(b) shows the k-space representation of the exciton's modulus square, being it mainly located in one point of the k-mesh. Figures 3(c) and (d) present real space side and top views, respectively, of the first peak excitonic wave function obtained from the calculations. The exciton, with a radius of approximately 3 nm, spans several lattice constants, reflecting the strong localization in reciprocal space around the K and K′ valleys. Consequently, a dense k-mesh is necessary to mitigate spurious Coulomb repulsion between periodic excitons.

Notably, fig. 3(d) illustrates that the exciton wave function extends beyond the Bi monolayer, reaching at least two atomic layers into the SiC substrate.

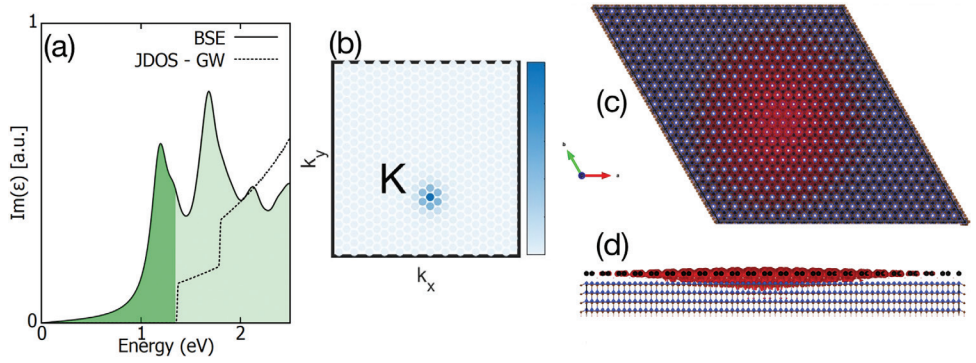

Fig. 3. – (a) Ab-initio GW+BSE absorption spectrum for Bi:SiC. The dashed line represents the joint density of states (JDOS) derived from the G_0W_0 calculation, with the omission of electron-hole interaction. Upon inclusion of the latter interaction, within the BSE framework, the absorption spectrum changes significantly, both qualitative and quantitative. The spectrum lying within the G_0W_0 direct gap ($\sim 1.35\,\mathrm{eV}$) has been highlighted with a darker tone of green. (b) Modulus square of the excitonic wave function, plotted in k-space. Only a section of the Brillouin Zone is shown here. Note the pronounced localization around the K/K$'$ point. (c) Top view of the A exciton wave function in real space, whose radius is about 3 nm. (d) Lateral view of the wave function in real space. Note its deep penetration into the substrate.

This underscores the critical role played by the substrate in Bi:SiC at both single- and two-particle levels. SiC not only contributes to the orbital filtering mechanism and the substantial topological gap, but also serves as a crucial screening channel for the Coulomb interaction [4, 6].

4. – Conclusions

In conclusion, this work focuses on the theoretical aspects on the observation of excitons in a large-gap and atomically thin QSH insulator [1]. Especially it addresses the first detection of excitons in an experimentally achievable topological insulator.

Two significant optical transitions become evident in the many-particle response of Bi:SiC, as soon as the electron-hole interactions are considered via the Bethe-Salpeter equation (fig. 3(a)). These are associated to the excitonic transitions from the Rashba-split valence bands at the K/K$'$ point (fig. 3(b)). In particular, only the lowest excitonic peak is embedded into the single-particle direct gap, and has a binding energy of $\sim$ 0.15 eV. The other peak, instead, is already embedded into the continuum.

The fundamental role played by the SiC substrate is highlighted, which not only influences the electronic and mechanical properties of the compound by filtering out the Bi p_z orbitals, but also breaks the inversion symmetry, opens a huge topological gap, and stabilizes the structure [4, 6]. The substrate also provides a screening channel for the Coulomb interaction.

Finally it is observed that, in Bi:SiC, both excitons and topology originate from the same electronic states. In this way, it is established a connection between excitonic and topological physics, which so far has only been proposed theoretically [20].

The reader interested in the experimental side of the work, especially concerning room-temperature aspects, can refer to [1].

* * *

The author acknowledges Marcin Syperek, Raul Stühler, PawełHolewa, PawełWyborski, Łukasz Dusanowski, Felix Reis, Sven Höfling, Ronny Thomale, Werner Hanke, Ralph Claessen, Domenico Di Sante and Christian Schneider for the contributions to the original publication [1]. The author further acknowledges the Gauss Centre for Supercomputing e.V. (`https://www.gauss-centre.eu`) for funding this project by providing computing time on the GCS Supercomputer SuperMUC-NG at Leibniz Supercomputing Centre (`https://www.lrz.de`) and the funding support from the Deutsche Forschungsgemeinschaft (DFG, German Research Foundation) under Germany's Excellence Strategy through the Würzburg-Dresden Cluster of Excellence on Complexity and Topology in Quantum Matter ct.qmat (EXC 2147, Project ID 390858490) as well as through the Collaborative Research Center SFB 1170 ToCoTronics (Project ID 258499086).

REFERENCES

[1] Syperek M., Stühler R., Consiglio A. *et al.*, *Nat. Commun.*, **13** (2022) 6313.
[2] Mueller T. and Malic E., *npj 2D Mater. Appl.*, **2** (2018) 29.
[3] Chernikov A. *et al.*, *Phys. Rev. Lett.*, **113** (2014) 076802.
[4] Reis F. *et al.*, *Science*, **357** (2017) 287.
[5] Wu S. *et al.*, *Science*, **359** (2018) 76.
[6] Li G., Hanke W., Hankiewicz E. M., Reis F., Schäfer J., Claessen R., Wu C. and Thomale R., *Phys. Rev. B*, **98** (2018) 165146.
[7] Giannozzi P. *et al.*, *J. Phys.: Condens. Matter*, **21** (2009) 395502.
[8] Perdew J. P., Burke K. and Ernzerhof M., *Phys. Rev. Lett.*, **77** (1996) 3865.
[9] Hedin L., *Phys. Rev.*, **139** (1965) A796.
[10] Strinati G., Mattausch H. J. and Hanke W., *Phys. Rev. Lett.*, **45** (1980) 290.
[11] Strinati G., Mattausch H. J. and Hanke W., *Phys. Rev. B*, **25** (1982) 2867.
[12] Strinati G., *Riv. Nuovo Cimento*, **11** (1988) 1.
[13] Hanke W. and Sham L. J., *Phys. Rev. B*, **12** (1975) 4501.
[14] Hanke W. and Sham L. J., *Phys. Rev. Lett.*, **43** (1979) 387.
[15] Rohlfing M. and Louie S. G., *Phys. Rev. Lett.*, **81** (1998) 2312.
[16] Sangalli D. *et al.*, *J. Phys. Condens. Matter*, **31** (2019) 325902.
[17] Marini A., Hogan C., Grüning M. and Varsano D., *Comput. Phys. Commun.*, **180** (2009) 1392.
[18] Momma K. and Izumi F., *J. Appl. Cryst.*, **41** (2008) 653.
[19] Hanke W., *The role of electron-hole interaction in the optical spectra of semiconductors and insulators*, in *Festkörperprobleme 19* (Springer) 1979, p. 43.
[20] Blason A. and Fabrizio M., *Phys. Rev. B*, **102** (2020) 035146.